J. Phys. G: Nucl. Part. Phys. **36** (2009) 035201 (12pp) doi:10.1088/0954-3899/36/3/035201

A test of the hadronic interaction model EPOS with air shower data

W D Apel[1], J C Arteaga[1,10], F Badea[1], K Bekk[1], M Bertaina[2], J Blümer[1,3], H Bozdog[1], I M Brancus[4], M Brüggemann[5], P Buchholz[5], E Cantoni[3,6], A Chiavassa[2], F Cossavella[3], K Daumiller[1], V de Souza[3,11], F Di Pierro[2], P Doll[1], R Engel[1], J Engler[1], M Finger[1], D Fuhrmann[7], P L Ghia[6], H J Gils[1], R Glasstetter[7], C Grupen[5], A Haungs[1], D Heck[1], J R Hörandel[3,12,13], T Huege[1], P G Isar[1], K-H Kampert[7], D Kang[3], D Kickelbick[5], H O Klages[1], Y Kolotaev[5], P Luczak[8], H J Mathes[1], H J Mayer[1], J Milke[1], B Mitrica[4], C Morello[6], G Navarra[2], S Nehls[1], J Oehlschläger[1], S Ostapchenko[1,14], S Over[5], M Petcu[4], T Pierog[1], H Rebel[1], M Roth[1], H Schieler[1], F Schröder[1], O Sima[9], M Stümpert[3], G Toma[4], G C Trinchero[6], H Ulrich[1], J van Buren[1], W Walkowiak[5], A Weindl[1], J Wochele[1], M Wommer[1] and J Zabierowski[8]

[1] Institut für Kernphysik, Forschungszentrum Karlsruhe, 76021 Karlsruhe, Germany
[2] Dipartimento di Fisica Generale dell'Università, 10125 Torino, Italy
[3] Institut für Experimentelle Kernphysik, Universität Karlsruhe, 76021 Karlsruhe, Germany
[4] National Institute of Physics and Nuclear Engineering, 7690 Bucharest, Romania
[5] Fachbereich Physik, Universität Siegen, 57068 Siegen, Germany
[6] Istituto di Fisica dello Spazio Interplanetario, INAF, 10133 Torino, Italy
[7] Fachbereich Physik, Universität Wuppertal, 42097 Wuppertal, Germany
[8] Soltan Institute for Nuclear Studies, 90950 Lodz, Poland
[9] Department of Physics, University of Bucharest, 76900 Bucharest, Romania

E-mail: j.horandel@astro.ru.nl

Received 3 November 2008
Published 4 February 2009
Online at stacks.iop.org/JPhysG/36/035201

Abstract

Predictions of the hadronic interaction model EPOS 1.61 as implemented in the air shower simulation program CORSIKA are compared to observations with the KASCADE experiment. The investigations reveal that the predictions of EPOS are not compatible with KASCADE measurements. The discrepancies seen are most likely due to use of a set of inelastic hadronic cross sections that are too high.

(Some figures in this article are in colour only in the electronic version)

[10] Present address: Institute of Physics and Mathematics, Universidad Michoacana, Morelia, Mexico.
[11] Present address: Universidade de São Paulo, Instituto de Fisica de São Carlos, Brazil.
[12] Author to whom any correspondence should be addressed.
[13] Present address: Department of Astrophysics, Radboud University Nijmegen, The Netherlands.
[14] Present address: Norwegian University, Trondheim, Norway.

1. Introduction

When high-energy cosmic rays penetrate the Earth's atmosphere they initiate cascades of secondary particles—the extensive air showers. Objective of air shower detectors is to derive information about the shower inducing primary particle from the registered secondary particles. Addressing astrophysical questions with air shower data necessitates the understanding of high-energy interactions in the atmosphere. Or, in reversion, the interpretation of properties of primary radiation derived from air shower measurements depends on the understanding of the complex processes during the development of air showers. In the last decade significant progress has been made in the interpretation of air shower data and main properties of the primary cosmic radiation have been measured. At energies around 10^6 GeV the mass composition of cosmic rays has been investigated and energy spectra for groups of elements could be derived [1, 2]. It could be shown that the knee in the all-particle energy spectrum at about 4×10^6 GeV is caused by a cut-off in the energy spectra of the light elements (protons and helium). Despite this progress, detailed investigations indicate inconsistencies in the interpretation of air shower data [1, 3–8]. Thus, one of the goals of KASCADE (Karlsruhe Shower Core and Array DEtector) is to investigate high-energy interactions in the atmosphere and to improve contemporary models to describe such processes.

For air shower interpretation the understanding of multi-particle production in hadronic interactions with a small momentum transfer is essential [9]. Due to the energy dependence of the coupling constant α_s soft interactions cannot be calculated within QCD using perturbation theory. Instead, phenomenological approaches have been introduced in different models. These models are the main source of uncertainties in simulation codes to calculate the development of extensive air showers, such as the program CORSIKA [10]. Several codes to describe hadronic interactions at low energies ($E < 200$ GeV; e.g. GHEISHA [11] and FLUKA [12, 13]) as well as high energies (e.g. DPMJET [14], QGSJET [15–17], SIBYLL [18] and EPOS [19, 20]) have been embedded in CORSIKA.

The testing of interaction models necessitates detailed measurements of several shower components. The KASCADE experiment [21] with its multi-detector set-up, registering simultaneously the electromagnetic, muonic and hadronic shower components is particularly suited for such investigations. The information derived on properties of high-energy interactions from air shower observations is complementary to measurements at accelerator experiments since different kinematical and energetic regions are probed.

In previous investigations [7, 8] the models QGSJET versions 98 and 01 [15], VENUS [22], SIBYLL versions 1.6 [23] and 2.1 [18], DPMJET [14] and NEXUS [24] have been studied. The analyses presented in this paper focus on the interaction model EPOS, version 1.61. This model is a recent development, historically emerging from the VENUS and NEXUS codes.

EPOS is a consistent quantum mechanical multiple scattering approach based on partons and strings, where cross sections and the particle production are calculated consistently, taking into account energy conservation in both cases (unlike other models where energy conservation is not considered for cross section calculations [25]). A special feature is the explicit treatment of projectile and target remnants, leading to a better description of baryon and antibaryon production than in other models used for cosmic-ray analysis. Motivated by the data obtained by the RHIC experiments, nuclear effects related to Cronin transverse momentum broadening, parton saturation, and screening have been introduced into EPOS. Furthermore, unlike other models, high-density effects leading to collective behavior in heavy-ion collisions (or lighter systems) are also taken into account. Since this model is applied to accelerator physics, many data are considered which are not *a priori* linked to cosmic rays and air

showers. That is maybe the largest difference to all other hadronic models used to simulate air showers.

2. Experimental set-up

2.1. The apparatus

The experiment KASCADE, located on site of the Forschungszentrum Karlsruhe, 110 m a.s.l., consists of several detector systems. A description of the performance of the experiment can be found elsewhere [21]. A 200×200 m^2 array of 252 detector stations, equipped with scintillation counters, measures the electromagnetic and, below a lead/iron shielding, the muonic parts of air showers. In its center, an iron sampling calorimeter of 16×20 m^2 area detects hadronic particles. The calorimeter is equipped with 11 000 warm-liquid ionization chambers arranged in nine layers. Due to its fine segmentation (25×25 cm^2), energy, position and angle of incidence can be measured for individual hadrons. A detailed description of the calorimeter and its performance can be found in [26]; it has been calibrated with a test beam at the SPS at CERN up to 350 GeV particle energy [27].

2.2. Observables and event selection

The position of the shower axis and the angle of incidence of a cascade are reconstructed by the array detectors. The total numbers of electrons N_e and muons N_μ are determined by integrating their lateral distributions. In the case of muons, the truncated muon number N_μ^{tr} is used for experimental reasons. It is the number of muons integrated in the distance range 40–200 m from the shower axis. For a detailed description of the reconstruction algorithms see [28]. The position of the shower axis is reconstructed with an accuracy better than 2 m and the angle of incidence better than 0.5°.

The hadrons in the calorimeter are reconstructed by a pattern recognition algorithm, optimized to recognize as many hadrons in a shower core as possible. Details can be found in [28]. Hadrons of equal energy can still be separated with a probability of 50% at a distance of 40 cm. The reconstruction efficiency rises from 70% at 50 GeV to nearly 100% at 100 GeV. The energy resolution improves from 30% at 50 GeV to 15% at 10^4 GeV. The hadron number N_h and hadronic energy sum $\sum E_h$ are determined by the sum over all hadrons in a distance up to 10 m from the shower axis. A correction for the missing area beyond the boundaries of the calorimeter is applied. In the following, N_h and $\sum E_h$ are given for a threshold of 100 GeV, but also hadronic shower sizes for higher thresholds up to 500 GeV have been investigated. The observable $\sum E_h$ includes also energy of hadrons which could not be reconstructed independently, because they are too close to each other. It shows up in the simulated and experimental data in the same manner.

To be accepted for the analysis, an air shower has to fulfil several requirements: at least one hadron has been reconstructed in the calorimeter with an energy larger than 50 GeV, the shower axis is located inside the calorimeter, the electromagnetic shower size N_e is larger than 10^4, the truncated muon number N_μ^{tr} is larger than 10^3, i.e. the primary energy is greater than about 3×10^5 GeV, and the reconstructed zenith angle is smaller than 30°. For figures 2 and 6 different selection criteria have been applied [1]. Namely: the reconstructed shower axis has to be within 91 m from the center of the array, the age parameter s, obtained through a fit of an NKG function to the lateral distribution of the electromagnetic component has to be in the interval $0.2 < s < 2.1$, and only showers with $\lg N_e \geqslant 4.8$, $\lg N_\mu^{\mathrm{tr}} \geqslant 3.6$, as well as a zenith angle $<18°$ are considered.

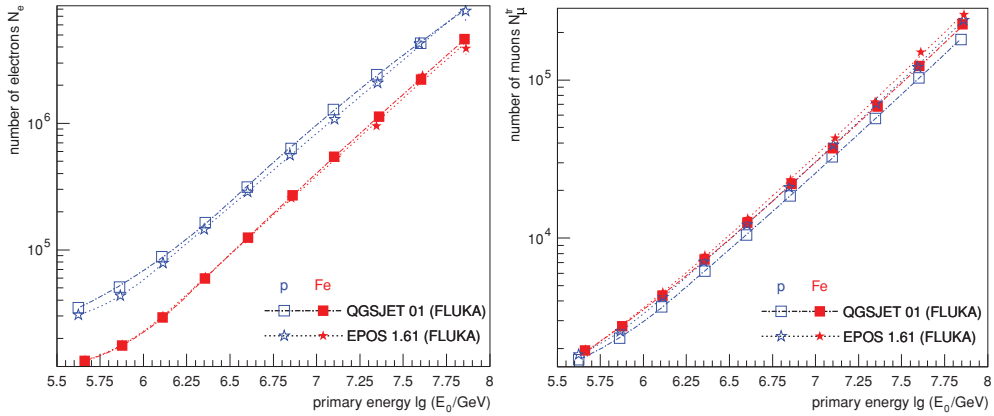

Figure 1. Number of electrons (left) and number of muons (right) as a function of shower energy for proton and iron-induced showers as predicted by the hadronic interaction models EPOS and QGSJET 01.

2.3. Simulations

The shower simulations were performed using CORSIKA. Hadronic interactions at low energies were modeled using the FLUKA code [12, 13]. High-energy interactions were treated with EPOS 1.61 [19, 20] ($E > 80$ GeV) as well as QGSJET 01 [15] ($E > 200$ GeV). The latter has been chosen for reference in order to compare the results discussed in the present paper to previous publications [7, 8]. Showers initiated by primary protons and iron nuclei have been simulated. The simulations covered the energy range 10^5–10^8 GeV with zenith angles in the interval 0°–32°. The spectral index in the simulations was −2.0. For the analysis it is converted to a slope of −2.7 below and −3.1 above the knee with a rigidity-dependent knee position (3×10^6 GeV for protons)[15]. The positions of the shower axes are distributed uniformly over an area exceeding the calorimeter surface by 2 m on each side. In order to determine the signals in the individual detectors, all secondary particles at the ground level are passed through a detector simulation program using the GEANT package [29]. In this way, the instrumental response is taken into account and the simulated events are analyzed by the same code as the experimental data, an important aspect to avoid biases by pattern recognition and reconstruction algorithms.

The average primary energy belonging to a simulated and reconstructed number of electrons and muons is given in figure 1. The left panel demonstrates the N_e dependence on the primary mass. The lines through the points are drawn to guide the eye and represent five parameter fits. As in all figures errors of the mean values are plotted. But, in most cases, the error bars are smaller than the marker size. It is seen from figure 1 that both models yield a nearly linear dependence. Only near threshold does N_e rise slowly for light primaries, namely protons. The number of muons is expected to be a good estimator for the primary energy, since, irrespective of the individual shower development, the most abundant secondaries of the interactions are pions, for which the charged species decay to muons and arrive to a large extent at the Earth's surface. This behavior is illustrated in figure 1 (right). The difference in energy for protons and iron nuclei for a fixed number of muons amounts to about 25% only for both models.

[15] Again, figures 2 and 6 have been treated differently, see [1].

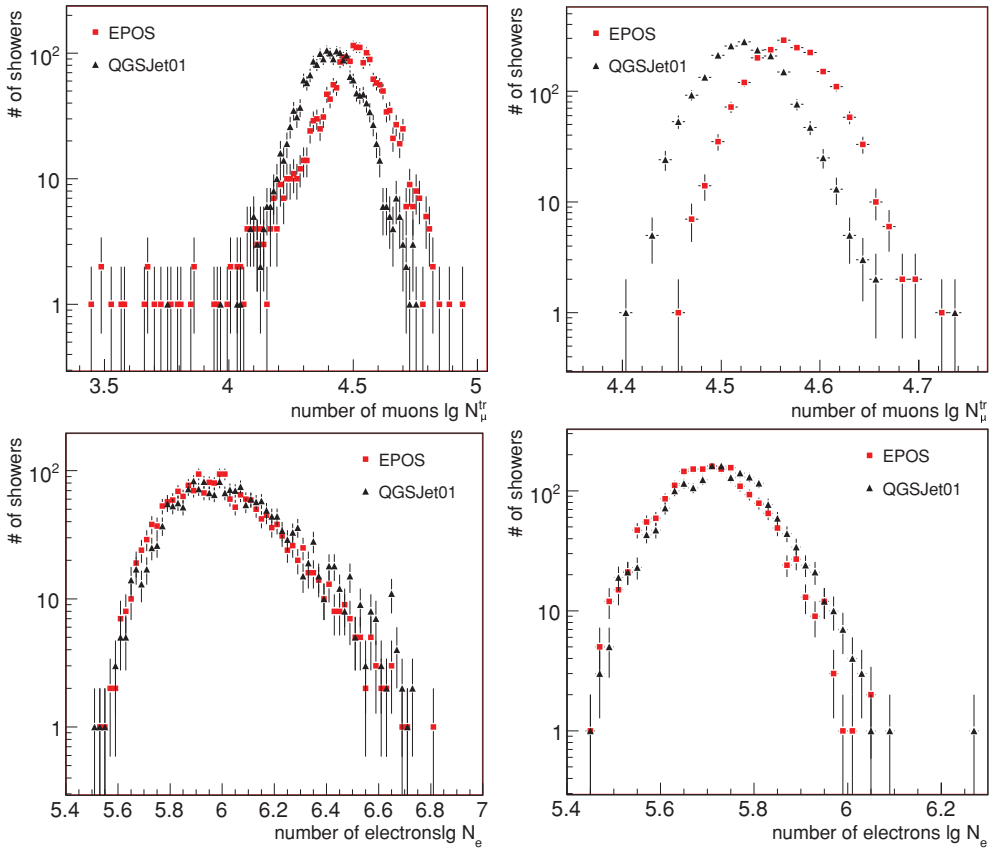

Figure 2. Predictions of two interaction models for the number of registered muons (top) and electrons (bottom) at the ground for primary protons (left) and iron nuclei (right) with an energy of 10^7 GeV.

3. Results

3.1. Primary energy correlations

The number of electrons and muons registered at the ground level as a function of energy for the interaction models EPOS 1.61 and QGSJET 01 is depicted in figure 1. For protons differences between the predictions of the two models can be recognized. These differences are less pronounced for iron-induced showers. The number of electrons is slightly lower for a fixed energy for the model EPOS and the number of muons is larger for this model as compared to QGSJET.

While mean values are shown in figure 1, the underlying distributions are given in figure 2. The figure displays the number of muons (top) and electrons (bottom) expected for showers with an energy of 10^7 GeV for primary protons (left) and iron nuclei (right). Results for EPOS are compared to predictions of the model QGSJET 01. For both primary particle species EPOS yields clearly more muons at the observation level as compared to QGSJET, while the shapes of the distributions are very similar. The corresponding distributions for the number of electrons observed at the ground level are very similar for both models. They agree

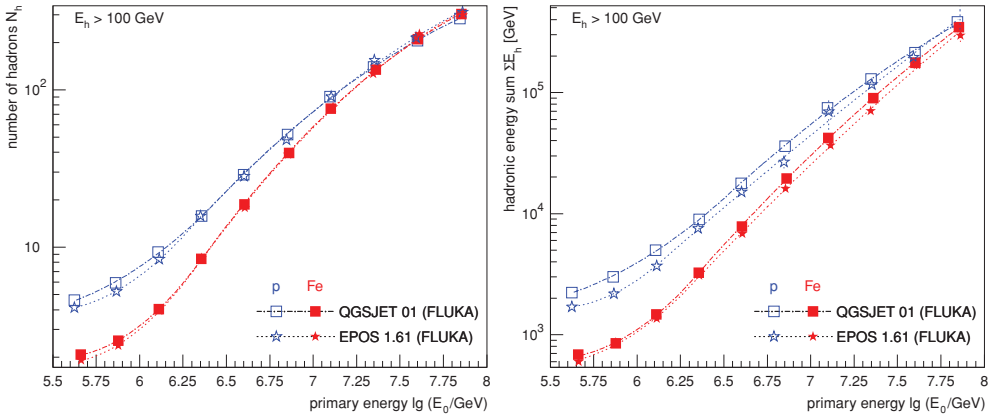

Figure 3. Number of hadrons (left) and hadronic energy sum (right) as a function of shower energy for two interaction models and two primary particle species.

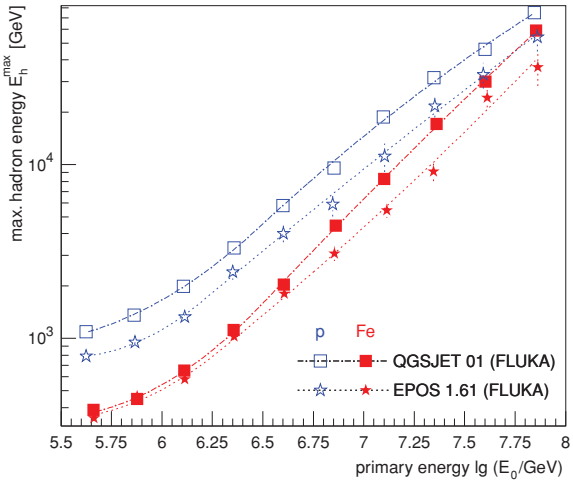

Figure 4. Energy of the most energetic hadron in a shower as a function of shower energy for two interaction models and two primary particle species.

well in shape for both, primary protons and iron nuclei. But the positions of the maxima are slightly shifted.

The relations of observed hadronic observables as a function of shower energy are presented in figures 3 and 4. They show the numbers of hadrons N_h, the hadronic energy sum $\sum E_h$ and the energy of the highest energy hadron observed at ground $E_h^{\max}$, respectively. The numbers of hadrons for a given energy predicted by both, EPOS and QGSJET 01 are very similar. But there is a significant difference in the hadronic energy transported to the observation level. EPOS yields about 25% smaller values for $\sum E_h$ as compared to QGSJET 01 at the same shower energy. The effect has a similar magnitude for both primary species. An even bigger difference is observed for the value of the highest energy hadron registered at the ground level. The maximum energies are reduced by up to 50% to 60% for EPOS compared

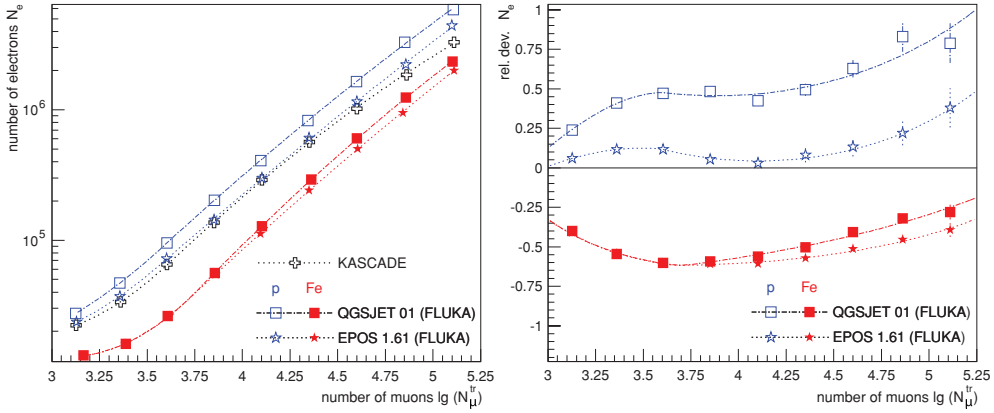

Figure 5. Number of electrons as a function of muons for model predictions compared to KASCADE measurements. Absolute values (left) and relative values $(N_e^{\mathrm{sim}} - N_e^{\mathrm{meas}})/N_e^{\mathrm{meas}}$ (right). Predictions for two interaction models and two primary particle species are shown.

to QGSJET at the same shower energy. Again, the effect is similarly strong for both primary species.

3.2. Electron–muon correlations

Turning our attention toward observable quantities, among the most interesting ones is the effect of the different models on the number of electrons and muons at the ground level. They are used to reconstruct energy and mass of the shower-inducing particles, e.g. by applying an unfolding algorithm [1, 30].

The average number of electrons as a function of the number of muons is displayed in figure 5 (left) for the two models. Predictions for primary protons and iron nuclei are compared to measured values. To emphasize the differences between the model predictions, the same data are plotted on the right hand panel in a different manner. The model predictions are shown relative to the measured values, i.e. the quantity $\left(N_e^{\mathrm{sim}} - N_e^{\mathrm{meas}}\right)\big/N_e^{\mathrm{meas}}$ is presented. For a given muon number EPOS clearly yield less electrons ($\approx$40%) for proton-induced cascades and significantly lesser electrons for iron showers at high energies, i.e. large muon numbers. This can be understood taking figure 1 into account. The differences seen there for given primary energies translate into the significant discrepancies between the two models seen in the electron–muon correlation (figure 5).

To estimate the effects on the unfolding procedure it is useful to have a look at the N_e–N_μ plane, see figure 6. The figure represents the measured two-dimensional shower size spectrum (grey coded area). The lines correspond to most probable values for primary protons and iron nuclei as predicted by the interaction models EPOS and QGSJET. It can clearly be recognized that the lines for EPOS are shifted toward the lower right corner of the figure with respect to QGSJET. This implies, if EPOS predictions are used to derive the mass of the primary particles from the observed data a dominantly light mass composition is obtained.

To check this effect, the energy spectra for five groups of elements (as in [1]) have been unfolded from the measurements, based on EPOS predictions. In this exercise in the energy range between 10^6 and 10^7 GeV a very high flux of protons is obtained and the flux of heavy particles (iron group) is strongly suppressed. If one extrapolates direct measurements to high

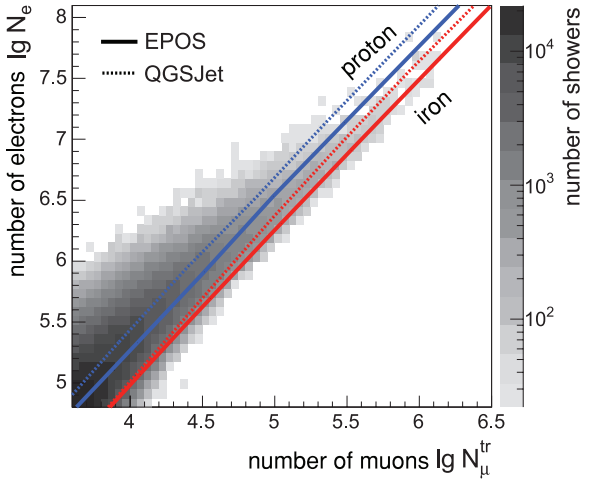

Figure 6. Number of electrons as a function of muons ($N_e - N_\mu$ plane). The measured two-dimensional shower size distribution (grey shaded area) is compared to most probable values as predicted by two interaction models for two primary species.

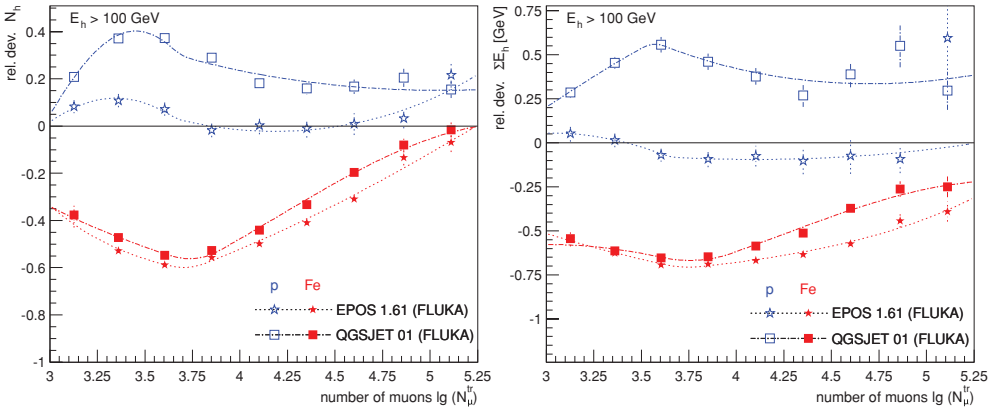

Figure 7. Number of hadrons observed (left) and reconstructed hadronic energy sum (right) as a function of the registered number of muons for proton and iron-induced showers. The predictions of two interaction models are shown relative to the measured values.

energies, such behavior seems to be extremely unrealistic. This study illustrates that it would be very useful to measure the energy spectra of individual elements directly up to the knee region. Such data would be very helpful to verify the interaction codes utilized in air shower simulations.

3.3. Hadron–muon correlations

The differences already seen in figure 3 are not directly accessible in measurements, since the energy of the primary particle cannot be inferred directly. To check the validity of interaction models it is therefore suitable to plot observable quantities against each other such as e.g. the number of registered hadrons or the observed hadronic energy at the ground level as a function of the number of muons as depicted in figure 7. Again, the model predictions are

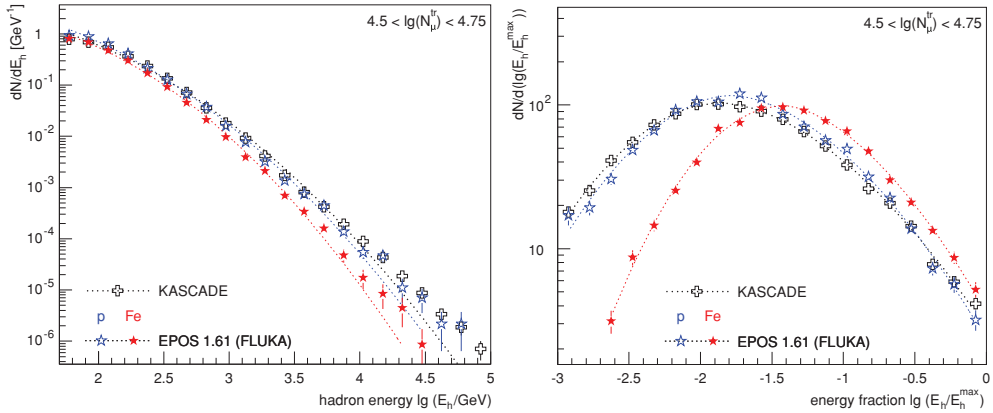

Figure 8. Energy spectrum of reconstructed hadrons (left) and fraction of the reconstructed hadron energy to the maximum hadron energy (right) for a given muon number interval. EPOS predictions for proton and iron-induced cascades are compared to measured values.

plotted relative to the values measured by KASCADE, i.e. the quantity $(x_{\mathrm{sim}} - x_{\mathrm{meas}})/x_{\mathrm{meas}}$ is presented. x represents N_h or $\sum E_h$ for two interaction models and two primary particle species. In particular for primary protons for a given muon number EPOS yields significantly less hadrons and delivers less hadronic energy to the observation level. It is generally assumed that in the energy range of interest the average mass composition of cosmic rays is between protons and iron. Thus, in figure 7 (as in figure 5, right) the zero line should be 'bracketed' by the predictions for proton and iron-induced showers, as it is the case for the model QGSJET. On the other hand, it can be recognized that for EPOS at high muon numbers (corresponding to energies around 10^7 GeV) the hadronic energy sums of both, proton and iron-induced showers are smaller than the experimental data. The systematic uncertainty of the hadronic energy sum amounts to about 15%. Within this uncertainty the data are compatible with the EPOS predictions, assuming that all cosmic rays are protons only. However, at energies around 10^6–10^7 GeV this is not realistic. This implies that the EPOS predictions are not compatible with the data.

The behavior observed for the maximum hadron energy $E_h^{\max}$ registered at the observation level is very similar to the situation depicted in figure 7 (right) for the hadronic energy sum. At high muon numbers EPOS yields values for $E_h^{\max}$ which are clearly below the measurements for both primary species (protons and iron nuclei)—an unrealistic scenario.

Another way to shed light on the interaction models is to investigate the energy spectra of hadrons for a given muon number interval, i.e. an approximately fixed primary energy. Hadron energy spectra as predicted by EPOS are compared to measured values in figure 8 (left)[16]. The muon number interval corresponds to primary energies around 2×10^7 GeV. At high hadron energies EPOS underestimates the observed flux. The predictions for both primary species are below the measured values. This observation is compatible with the above findings (figures 3 and 4), namely the relatively low hadronic energy sum and the relatively small maximum hadron energy.

Distributions of the ratio of the energy of each reconstructed hadron to the maximum hadron energy in each shower $E_h \big/ E_h^{\max}$ are plotted in figure 8 (right) for the same muon

[16] The corresponding distributions for the interaction model QGSJET have been published previously [7] The predictions are compatible with the measured data.

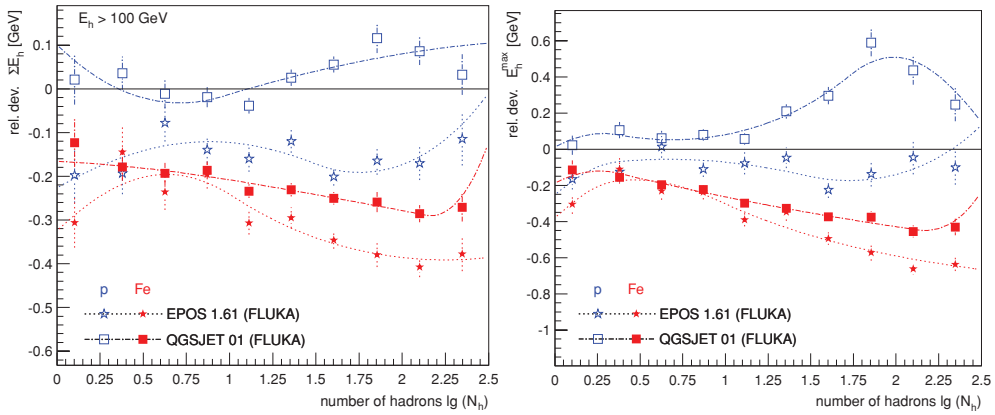

Figure 9. Relative hadronic energy sum $(\sum E_h^{\mathrm{sim}} - \sum E_h^{\mathrm{meas}})/\sum E_h^{\mathrm{meas}}$ (left) and relative maximum hadron energy (right) as a function of the reconstructed number of hadrons for two interaction models and two primary particle species.

interval as above. Again, EPOS predictions for two particle species are compared to measured data. As for the other observables discussed, the measurements should be 'bracketed' by the predictions for proton and iron-induced showers. However, the EPOS predictions exhibit clearly different behavior. For most $E_h \big/ E_h^{\max}$ ratios the measured values are outside the proton–iron range given by the model.

The investigations of the energy spectra confirm the above findings that EPOS predictions are not compatible with KASCADE data.

3.4. Hadron–hadron correlations

In the previous discussions it has already been seen that EPOS delivers less energy in the form of hadrons to the ground level as compared to QGSJET 01. Therefore, it is an interesting exercise to investigate also the correlations of the purely hadronic observables with each other. Examples of such correlations are presented in figure 9, depicting the hadronic energy sum (left) and the maximum hadron energy per shower (right). The predicted values are again plotted relative to the measured quantities to visually magnify the differences between the model predictions. In the figure the quantities are plotted as a function of the number of hadrons N_h. Due to the steeply falling energy spectrum and the $N_h - E_0$ correlation (see figure 3) a sampling of the data in N_h intervals yields an enrichment of light particles. Therefore, the data are expected to look very 'proton like'. Indeed, for QGSJET the proton predictions are very close to the 'zero line', i.e. to the KASCADE measurements. It should also be mentioned that (within the error bars) the QGSJET predictions 'bracket' the measured values. In contrast, the EPOS predictions for both primary species are below zero for both observables shown in the figure. The EPOS predictions for protons are at the lower bound of the 15% systematic uncertainty for the hadronic energy sum. Thus, they are barely compatible with the data. However, it should be stressed that the QGSJET predictions for protons really are at values around zero as expected. This indicates that the systematic effects might be smaller than estimated and the EPOS predictions are not compatible with the measurements. From all observables investigated the hadron–hadron correlations exhibit the strongest incompatibility between the EPOS predictions and the KASCADE data.

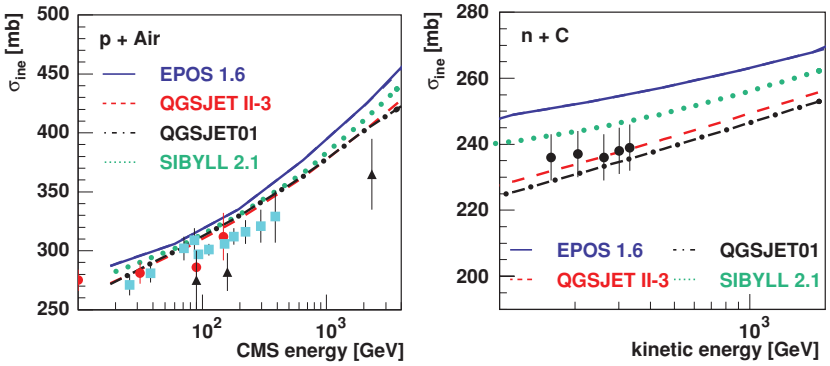

Figure 10. Inelastic cross sections for proton–air (left) and neutron–carbon (right) collisions as predicted by various interaction models. The symbols represent experimental data, left: KASCADE prototype calorimeter (dots) [31], Yodh *et al* (squares) [32], ARGO-YBJ (triangles $\sim$ 100 GeV) [33] and EAS-TOP (triangle $\sim$ 2000 GeV) [34]; right: Roberts *et al* [35].

4. Summary and conclusions

Predictions of air shower simulations using the CORSIKA code with the hadronic interaction models EPOS 1.61 and QGSJET 01 have been compared to measurements of the KASCADE experiment. Various observables of the electromagnetic, muonic and hadronic component have been investigated and the correlations between them have been analyzed. They have been used to check the compatibility of the EPOS predictions with the KASCADE measurements.

The findings can be summarized as follows. The investigations of the hadronic observables exhibit that EPOS does not deliver enough hadronic energy to the observation level and the energy per hadron seems to be too small. In the $N_e - N_\mu$ plane the EPOS showers are shifted to lower electron and higher muon numbers relative to QGSJET 01. When the mass composition of cosmic rays is derived from measured values this effect leads to a relatively light mass composition. In summary, there is a significant discrepancy between the EPOS (version 1.61) predictions and the KASCADE data. The EPOS predictions are not compatible with the measurements.

Most likely the incompatibility of the EPOS predictions with the KASCADE measurements is caused by too high inelastic cross sections for hadronic interactions implemented in the EPOS code. To illustrate this, the proton–air and neutron–carbon cross sections as predicted by different models are displayed in figure 10. It can be recognized that the EPOS 1.61 values mark the upper limit of the variations exhibited by the different models. Already at moderate energies in the 100 GeV regime a clear difference between the models is visible. In particular, the example of the neutron–carbon cross section illustrates that even at energies accessible to today's accelerator experiments, the models contain different descriptions of the inelastic hadronic cross sections. According to the authors of the EPOS code, a new version is in preparation with lower cross sections. It is expected that the predictions of this version are in better agreement with air shower data. Further studies shall be presented in a follow-up publication.

The results presented also underline the importance of measuring hadronic observables in air shower experiments. They provide the most sensitive available means of investigating the properties of hadronic interactions at very high energies and kinematical ranges to complement accelerator experiments.

Acknowledgments

The authors would like to thank the members of the engineering and technical staff of the KASCADE–Grande collaboration, who contributed to the success of the experiment. The KASCADE–Grande experiment is supported by the BMBF of Germany, the MIUR and INAF of Italy, the Polish Ministry of Science and Higher Education and the Romanian Ministry of Education and Research (grant CEEX 05-D11-79/2005).

References

[1] Antoni T *et al* 2005 *Astropart. Phys.* **24** 1
[2] Navarra G *et al* 2003 *Proc. 28th Int. Cosmic Ray Conf. (Tsukuba)* **1** 147
[3] Antoni T *et al* 2002 *Astropart. Phys.* **16** 245
[4] Swordy S P *et al* 2002 *Astropart. Phys.* **18** 129
[5] Hörandel J R 2003 *Astropart. Phys.* **19** 193
[6] Hörandel J R 2003 *J. Phys. G: Nucl. Part. Phys.* **29** 2439
[7] Antoni T *et al* 1999 *J. Phys. G: Nucl. Part. Phys.* **25** 2161
[8] Apel W D *et al* 2007 *J. Phys. G: Nucl. Part. Phys.* **34** 2581
[9] Engel R 2006 *Nucl. Phys.* B **151** 437
[10] Heck D *et al* 1998 *Report FZKA 6019, Forschungszentrum Karlsruhe*
[11] Fesefeldt H 1985 Report PITHA-85/02, RWTH Aachen
[12] Fasso A *et al* 2005 CERN-2005-10, INFN/TC-05/11, SLAC-R-773
[13] Fasso A *et al* 2003 arXiv:hep-ph/0306267
[14] Ranft J 1995 *Phys. Rev.* D **51** 64
[15] Kalmykov N N *et al* 1997 *Nucl. Phys.* B **52B** 17
[16] Ostapchenko S S 2006 *Phys. Rev.* D **74** 014026
[17] Ostapchenko S S 2006 *Nucl. Phys.* B **151** 143, 147
[18] Engel R *et al* 1999 *Proc. 26th Int. Cosmic Ray Conf. (Salt Lake City)* vol 1 pp 415
[19] Werner K, Liu F M and Pierog T 2006 *Phys. Rev.* C **74** 044902
[20] Pierog T and Werner K 2006 arXiv:astro-ph 0611311
[21] Antoni T *et al* 2003 *Nucl. Instrum. Methods* A **513** 490
[22] Werner K 1993 *Phys. Rep.* **232** 87
[23] Engel J *et al* 1992 *Phys. Rev.* D **46** 5013
[24] Drescher H J *et al* 2001 *Phys. Rep.* **350** 93
[25] Hladik M *et al* 2001 *Phys. Rev. Lett.* **86** 3506
[26] Engler J *et al* 1999 *Nucl. Instrum. Methods* A **427** 528
[27] Plewnia S *et al* 2006 *Nucl. Instrum. Methods* A **566** 422
[28] Antoni T *et al* 2001 *Astropart. Phys.* **14** 245
[29] Geant 3.21 detector description and simulation tool 1993 *CERN Program Library Long Writeup W5013, CERN*
[30] Ulrich H *et al* 2008 *Nucl. Phys.* B *Proc. Suppl.* **175–6** 273
[31] Mielke H H *et al* 1994 *J. Phys. G: Nucl. Part. Phys.* **20** 637
[32] Yodh G B *et al* 1983 *Phys. Rev.* D **27** 1183
[33] Mitri I De *et al* 2007 *Proc. 30th Int. Cosmic Ray Conf. (Merida)* at press
[34] Aglietta M *et al* 2007 *Proc. 30th Int. Cosmic Ray Conf. (Merida)* at press
[35] Roberts T J *et al* 1979 *Nucl. Phys.* B **159** 56